第33卷第4期
2014年8月

红外与毫米波学报
J. Infrared Millim. Waves

Vol. 33, No. 4
August, 2014

文章编号:1001-9014(2014)04-0337-07

DOI:10.3724/SP.J.1010.2014.00337

# Design of the quasi-optical input launcher for 140 GHz gyrotron amplifier

CAI Jin-Chi[1,2], JIANG Yi[2], HU Peng[2], MA Guo-Wu[2], CHEN Hong-Bin[2], JIN Xiao[2], CHEN Huai-Bi[1]

(1. Department of Engineering Physics, Tsinghua University, Beijing 100084, China;
2. Institute of Applied Electronics, China Academy of Engenering Physics, Mianyang 621000, China)

**Abstract**: As a part of the innovative design of the 140 GHz gyrotron amplifier loaded with confocal waveguide, the design process of the quasi-optical input launcher is comprehensively demonstrated. Owing to the relative insensitivity of the Guassian optics to the frequency fluctuation, the bandwidth of this type of power coupler could be drastically larger than the typical inserted waveguide coupler. The input launcher comprised of the antenna coupler, the mirror transformer and corrugated waveguide guarantees 6.8 GHz bandwidth with respect to >50% power injection efficiency, solving the problem of parasitic resonances and unexpected efficiency shrink simultaneously.

**Key words**: gyrotron amplifier, quasi-optical launcher, power coupler
**PACS**: 07.50.-e, 07.57.Hm

# 140 GHz 回旋行波管放大器准光学注入结构的设计

蔡金赤[1,2], 蒋 艺[2], 胡 鹏[2], 马国武[2], 陈洪斌[2], 金 晓[2], 陈怀壁[1]

(1. 清华大学 工程物理系,北京 100084;
2. 中国工程物理研究院 应用电子学研究所,四川 绵阳 621000)

**摘要**:作为140 GHz共焦波导回旋行波管放大器设计中的一个创新部分,关于准光学注入结构的设计方法将详细论述.归因于高斯光束对频率扰动的欠敏感特性,这样的注入结构具有比传统波导插入耦合器更大的带宽.注入系统包括耦合天线、镜面变换器和波纹波导三个部分,最终在高于50%功率注入水平下达到6.8 GHz的带宽,并克服了可能的寄生模式振荡和由加工误差导致的注入效率迅速下降的问题.

**关 键 词**:回旋行波挂放大器;准光学注入结构;功率耦合器

**中图分类号**:TN802 **文献标识码**:A

## Introduction

The gyrotron amplifier is a high frequency vacuum electronic device to amplify the millimetre-wavelength microwave to the higher power levels with many prospected applications in terahertz regime. As a THz-amplifier, the two main obstacles supposed to be overcome are the large magnetic field (several Tesla) requirement and the parasitic mode oscillations when high order operating mode is used. The former problem could be handled by using high order harmonic electron-wave interaction principle. The latter problem is always solved by introducing additional power dissipation mechanism in purpose. Plating attenuating material onto the metallic wall or using Photonic Band Gap (PBG) structures are the most widely adopted methods so far. The confocal waveguide structure is proposed as another possible solution, which is composed of two face-to-face mirrors with the same curvature Rc and the distance equal to Rc, shown in Fig. 1.

It is easy to judge that all the modes in the confocal waveguide are gradually evanescent wave because the power leakage is unavoidable. The wall ohm power loss for microwave is negligible comparing with the diffraction power loss introduced deliberately. The $HE_{06}$ mode is selected as the operating mode since it has a much smaller power-loss rate than other modes to suppress the parasitic mode oscillation. Moreover, the high order mode selection

**Received date**: 2013-03-19, **revised date**: 2014-05-16 **收稿日期**:2013-03-19, **修回日期**:2014-05-16
**Foundation items**: Supported by Science Development Foundation of CAEP(2010-9090502B)
**Biography**: CAI Jin-Chi(1987-), male, Sichuan, China, PhD. Research fields focus on teraherdz technology. E-mail: caijinchino1@163.com

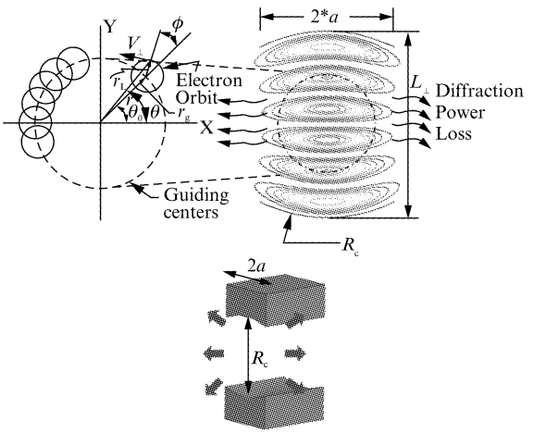


Fig. 1 Electric field of $HE_{06}$ mode in the confocal waveguide with, $R_c = L_\perp = 6.8$ mm, $a = 2.5$ mm

图1 $R = 6.8$ mm, $a = 2.5$ mm 的共焦波导中的 $HE_{06}$ 模式的电场分布

gives rise to a large enough dimension of cavity for permitting reasonable machining errors.

Based on particle-in-cell calculations, the gyrotron amplifier loaded with confocal waveguide structure was already designed by our group in a previous work, exhibiting excellent performance of high gain and large instantaneous frequency bandwidth with the assumption of the perfect input efficiency[1].

Stimulated by the MIT's primary work at input launcher design, a simply constructed power coupler modelled as Fig. 2[2] was carefully studied. The microwave is injected to the confocal waveguide from a circular waveguide which is inserted through one mirror of the confocal waveguide. The down-tapered structure at the entrance of the confocal waveguide ensures the microwave being sufficiently cut off to be reflected to the reverse direction and also makes space for the rotating electron beams to enter the confocal waveguide, as shown in Fig. 2.

To be disappointed, the bandwidth of this inserted-waveguide power coupler is too narrow to sustain the excellent bandwidth property of the whole amplifier system, with 50%-input-efficiency bandwidth of lower than 2 GHz, even though much effort has been done. Apart from the narrow bandwidth there are at least two disadvantages for this waveguide-inserted input launcher, as predieted by a theory. Firstly, since the transmission line also utilises up-tapered structure at the exit ends for the quasi-optical output[2], power is easily trapped in the tube with end reflections, causing parasitic resonance to disturb the expected amplification process. Secondly, this type of input launcher uses phase enhancement principle to achieve the high input efficiency at a specific frequency. Therefore, any fabrication irregularities will decrease the coupling efficiency in the form of reflection which has adverse impacts on the driving source. This phenomenon is already discussed and experimentally observed in MIT's gyrotron amplifier[3].

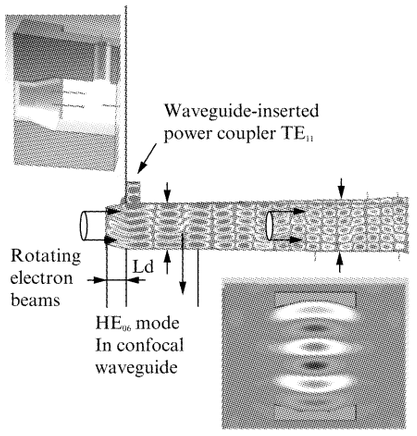


Fig. 2 Waveguide-inserted power coupler in MIT's gyrotron amplifier[2]

图2 MIT 设计的回旋放大器中插入波导的耦合结构[2]

For solving the above problems in the basic perspective, the conception of the quasi-optical injection with no down-tapered structure was initially put forward by Wen Hu in his Doctoral Dissertation[4]. The motivation has come from the recognition of some attractive characteristics of Gaussian optics. Firstly, the field distribution of the Gaussian beam changes insensitively when the frequency shifts and the beam waist dimension maintains. Second, the propagation of Gaussian could be considered as light beam in Geometric optics when the beam's transverse dimension is much larger than its wavelength.

Schematic CAD drawing of the confocal gyro-TWT amplifier's input system is shown in Fig. 3. It is obvious that this type of input launcher is more complexly constructed than the one shown in Fig. 2. The TE11 mode in circular waveguide is firstly transformed to round Gaussian beam through corrugated waveguide with longitudinal varied groove-depth. Then the round Gaussian beam is transformed to certain-transverse-distribution elliptical Gaussian beam though two surface-curved mirrors. Finally the elliptical Gaussian beam in the free space is transformed to HE06 mode in the confocal waveguide though antenna coupler component.

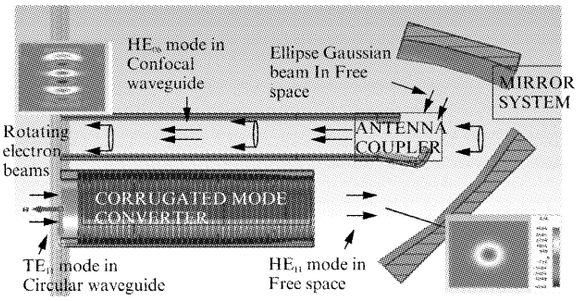


Fig. 3 CAD drawing of the confocal gyro-TWT amplifier's quasi-optical input system

图3 共焦波导结构的回旋行波管放大器的准光学注入注入结构图

Primary numeric result was given by C. D Joye in his PhD thesis[2], thus finally presenting the layout of the quasi-optical input launcher followed by this paper. There are at least two improvements when the quasi opti-

cal input launcher was adopted. Firstly, larger frequency bandwidth of the input efficiency has been achieved. Secondly, the reflection power caused by the irregularity in the tube is more likely to be leak and dissipated in the innovative input launcher other than trapped in the tube.

As the first attempt to provide the detailed description of this launcher, this paper focuses on the design issues of the three components mentioned above involving the antenna coupler, the corrugated mode converter and the mirror system, respectively. The main design process combines the analysis of the beam propagating path by geometric optics and the analysis of the field distribution along the path by Gaussian optics. A brief introduction to Gaussian transformation is presented in Chap. 2. The detailed optimization procedure of the three components is demonstrated in Chaps. 3 ~ 5. In the final chapter, the synthesis of the input launcher is given and some discussion and future prospect is then put forward.

## 1 Gaussian optics

Gaussian mode is an electro-magnetic mode which can exist in the free space just like the uniform planar wave. In its propagation direction, there is a specific cross section called the beam waist where the field only has transverse component and possesses the same phase. Generally, in all cross sections, the transverse electric field is vertical to the transverse magnetic field approximately with the same wave impendence of the TEM wave in the free space. The magnitude of the field decreases away from the centre in the Gaussian-function pattern[5]. In certain cross section, q parameters is defined to describe the field varying principle as Eq. 1, where $A(x, y, z)$ demonstrates any transverse field component in the form of complex amplitude:

$$A(x,y,z) = \frac{\text{constant}}{\sqrt{q_x(z)q_y(z)}} e^{-jkz} e^{\frac{kx^2}{2jq_x(z)}} e^{\frac{ky^2}{2jq_y(z)}} \quad . (1)$$

With the definition of $q$ parameters as a complex number, the Gaussian transformation could be easily described. With $qx = qy = js$ in Eq. 1, the beam waist of the round Gaussian beam could be derived. When the Gaussian beam passes the distance of d, the q parameter of both x and y direction will be changed as follow principle[5]:

$$q(z + d) = q(z) + d \quad . (2)$$

When the elliptical Guassian beam reflects on the mirror, with the assumption that $x$ orientation is parallel to the mirror plane and the y orientation is orthogonal direction to $x$ (for beams, also orthogonal to propagation direction), the $q$ parameter transformation could be written as Eq. 3[2,5]:

$$\frac{1}{q_y} = \frac{1}{q_{y0}} - \frac{2}{p_y/\cos\theta}, \quad \frac{1}{q_x} = \frac{1}{q_{x0}} - \frac{2}{p_x\cos\theta} \quad , (3)$$

where $\theta$ is the incident angle between the beam and norm directions of the mirror, $\rho_x$ and $\rho_y$ is the curvature of the mirror in two directions, $q_x$ and $q_y$ is the $q$ parameters of Gaussian beam in two directions. Since $q$ parameters determines the field distribution principle on Guassian beam, the field match issue relative to injection efficiency greatly depends on $q$ parameter design, which will be referred to many times in the following contents. Figure 4 demonstrates two special situations that clarify the definition of $x$ and $y$ directions in $q$ parameters and curvature of the mirrors.

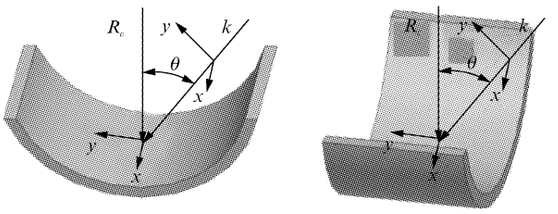


Fig. 4　The definition of $x$ and $y$ direction in Gaussian transformation on mirrors

图 4　镜面高斯变换中关于 $x$ 与 $y$ 方向的定义

## 2 Design of the antenna coupler

In this chapter, the configuration of antenna coupler and the parameters of the elliptical Guassian beam to be injected will be determined to optimize the injection efficiency. The antenna is actually the extension of the confocal mirrors, which has the same curvature but different width and complex profile of the longitudinal section. The 2-D geometrical shape in its longitudinal section is roughly presented in Fig. 5. Except the width of coupler, all the parameters of this antenna shown in Fig. 5 could be firstly derived from an equivalent planar model. The $q_y$ parameter of Gaussian beam will then be determined through Gaussian optics by analyzing $HE_{06}$ mode into Gaussian beam. The width is finally optimized by establishing a 3-D mode with other parameters already obtained by above process.

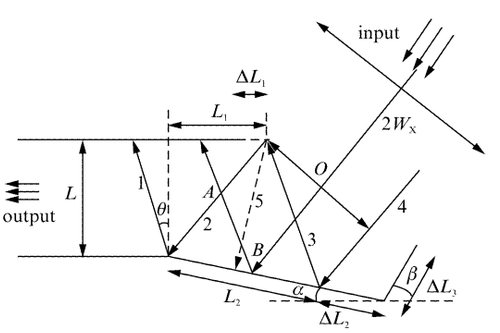


Fig. 5　The parameters of the perpendicular plane design

图 5　与电场垂直截面的尺寸设计示意图

With the consideration of the properties of millimetre microwave, light beams reflecting inside the waveguide are used to describe the propagation of $HE_{06}$ mode. Assuming that the phase changing rate in the beam direction equals that of the planar wave in the free space, the incident angle $\theta$ between the beam and norm directions of the mirror shown in Fig. 5 could be easily derived as Eq. 4:

$$\cos\theta = \lambda/\lambda_c \quad , (4)$$

$\lambda$ is free space wavelength and $\lambda_c$ is cut-off frequency of

$HE_{06}$ mode, which is equal to $0.32Rc$[2]. For our concerned frequency of 140 GHz, $\theta$ is roughly 10.0 degree. For simplifying the analysis, the planar waveguide with the distance of $L$ between the two plain mirrors is established to approximate the confocal waveguide with distance of R between the two curved mirrors with respect to the equivalent incident angle of $HE_{06}$ modes, which can be calculated by Eq. 4. The ratio of cut-off wavelength of $TE_{06}$ mode ($\lambda_{cp}$) in the planar waveguide to that of $HE_{06}$ mode in the confocal waveguide ($\lambda_{cc}$) can be written as Eq. 5[2]:

$$\lambda_{cp}/\lambda_{cc} = L/R_c \cdot 25/24 \quad . \quad (5)$$

The constant 25/24 is due to the curvature difference between the two types of mirrors. According to Eqs. 4 – 5 , with the equivalent incident angle at the same frequency, a 2-D equivalent model with all parameters multiplied by the factor of 24/25 is analyzed. With the solution of this 2-D injection problem, the factor of 25/24 should be resumed for confocal waveguide.

In the perspective of geometrical optics, parameters in Fig. 5 can be roughly set by geometrical method as initial values for further optimization. The goal is to design a light path to assure that when the light arrives at the confocal structure, the incident angle $\theta$ should be compatible with Eq. 4, thus achieving the best mode converting effect in general understanding.

As an intuitive imagination, the light beam identified by number 1, 2, 3, and 4 respectively, in Fig. 4 is used to determine $L_1$ and $L_2$, written as Eq. 6:

$$\begin{aligned} L_1 &= L\tan(\theta + 2\alpha) \\ L_2 &= L\frac{\cos\theta}{\cos(\theta + \alpha)}[\tan\theta + \tan(\theta + 2\alpha)] \end{aligned} \quad . \quad (6)$$

It should be emphasized that beam 2 is reflected onto the tilted antenna mirror to get beam 1, beam 4 is reflected onto the tilted antenna mirror to get beam 3, beam 2 and beam 3 have the common point, beam 3 is reflected onto the upper antenna mirror to get beam 5. Angle $\alpha$ is an arbitrary value in Eq. 6 which should be determined in the following analysis.

According to the further geometric analysis, when beam 5 is reflected onto the tilted mirror, the reflected beams cannot be parallel to beam 1 by adjusting nonzero angle $\alpha$. As an analogy to microwave cavity oscillations, angle $\alpha$ is determined to assure that the beam 5 could be perpendicular to the lower mirror, where the possible oscillation happens to lower the reflection power loss. Therefore, $\alpha$ and should be equal according to Geometric optics calculation in Fig. 5.

For efficient injection, the centre of the waist of Gaussian beam should be placed at point $O$, demonstrated as Fig. 5. The exact size of the beam waist is later to be determined by the numerical method. Generally speaking, with too large size adopted, the beam will be resisted by the upper mirror directly. However, with too small size, the Guassian beam will disperse drastically according to Guassian optics[5].

After above initial estimations, the preliminary parameters were obtained. It is obvious that those parameters could be optimized through more rigours numeric analysis. By establishing the 2-D numeric model to calculate the plane waveguide injection efficiency, an accurate design can be obtained very quickly, as shown in Table 1. $\Delta L_1$、$\Delta L_2$、$\Delta L_3$ represent the adjustment to the structure, shown in Fig. 5. As a result of the numeric calculation, all the parameters given above are adjusted a little to achieve the highest $|S_{21}|$ (through input to output) in its operation frequency. The angle $\beta$ is primarily set to make sure that the taper is parallel to the incident beams to restore reflection power as much as possible, given the value $\pi/2 - \theta - 2\alpha$.

**Table 1 Parameters of the perpendicular plane**
**表1 垂直平面各尺寸参数**

| $\theta$/° | $\alpha$/° | $\beta$/° | $L_1+\Delta L_1$/mm | $L_2+\Delta L_2$/mm | $\Delta L_3$/mm | $q_x$/mm |
|---|---|---|---|---|---|---|
| 10 +0.5 | 10 +0.5 | 60 –3 | 3.93 –0.02 | 5.37 +1.13 | 2.24 | j11.91 |

The parameters of parallel plane is designed on the basis of the parameters above where the $q_y$ parameter of Gaussian beam along another orientation (vertical to the paper) and the antenna width is to be achieved. $q_y$ at the point of $O$ is determined to make the $q_y$ at point A in Fig. 5 equals to $q_y$ at the confocal axis with reference to its $HE_{06}$ mode, as shown in Eq. 7[6], referred to Fig. 6.

$$q_A = j\frac{R}{2\cos\theta} \quad . \quad (7)$$

According to the Gaussian optics introduced in Chapter 2, it is not difficult to derive Eq. 8:

$$\frac{1}{q_y + OB} - \frac{2}{R/\cos(\alpha + \theta)} = \frac{1}{q_A - AB} \quad . \quad (8)$$

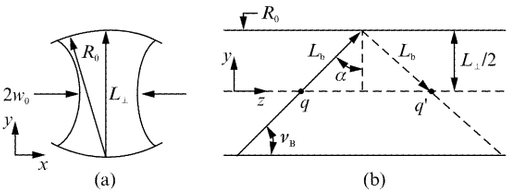


Fig. 6 $HE_{06}$ mode analyzed with Guassian beam
图6 用高斯光束分析的 $HE_{06}$ 模式

In our case, $q_y = -2.93 + j3.80$ mm. The next step is to determine the width of the antenna, as 2b in Fig. 7. The 3-D model is established to get a whole estimation of the design of the antenna coupler. By increasing the width of antenna, the power diffraction decreases whereas

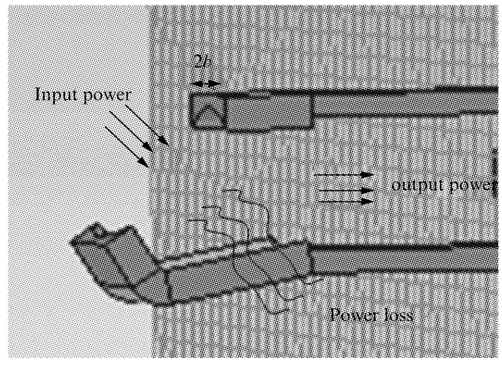


Fig. 7 3D model of the antenna coupler
图7 耦合天线的三维结构

the mismatched reflection increases. Therefore, there is the optimal half width $b = 3.6$ mm to obtain a highest the efficiency, by sweeping the parameters of $b$. At the frequency of 140 GHz, this optimized input efficiency for the antenna coupler alone is about 75% and the >50%-efficiency bandwidth is over 10 GHz.

## 3 Design of the corrugated mode converter

Considering the $TE_{11}$ mode of the cylindrical waveguide can be easily stimulated by the microwave source, the mode converter with corrugated wall is applied to convert the $TE_{11}$ mode to the Guassian-like radiation, as shown in Fig. 8.

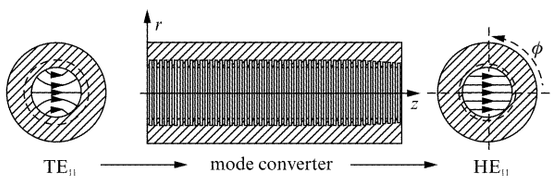


Fig. 8　Corrugated mode converter from $TE_{11}$ mode to $HE_{11}$ mode
图 8　$TE_{11}$ 模式到 $HE_{11}$ 模式的波纹波导转换结构

This converter comprises of the varying-depth-groove section and the uniform-depth-groove section. The former part converts $TE_{11}$ mode in the smooth wall waveguide to $HE_{11}$ mode and the later part supports the $HE_{11}$ mode to propagate independently in it for the radiation to the free space at the exit of the converter.

According to the anisotropic surface impedance theory[7], the overmoded corrugated waveguide with the large enough diameter of 10 mm, $1/4\lambda$ groove depth of 0.54 mm, corrugated period of 0.5 mm, and groove width of 0.25 mm is able to support the $HE_{11}$ Guassian-like mode to propagate independently at the frequency of 140 GHz. The round Guassian beam with the q parameter of j15.25 mm is then designed to emit at its exit port. It should be taken in mind that too large waveguide diameter cannot be adopted to reduce the difficulty in the mirror system design to be introduced in the next chapter. It would be better that the q parameter of the round Gaussian beam generated by this corrugated mode converter is similar to the qx and qy calculated in Chap. 3.

In order to convert the $TE_{11}$ mode in the smooth-surface waveguide with the diameter of 10 mm to the $HE_{11}$ mode in the corrugate waveguide with the above designed parameters, the depth of the groove should be varied from $\lambda/2$ to $\lambda/4$. The principle of the variation can be written as Eq. 9[8]:

$$d(z) = \frac{\lambda}{2} - \frac{\lambda}{4}\left(\frac{z}{L}\right)^N \quad , \quad (9)$$

where $L$ is the length of the transition section. With the goal to match the expected Guassian beam at the corrugated waveguide exit port as much as possible, the vector angle $\varphi$ with the respect of function scalar product between the simulated distribution and the provided Guassian distribution should be minimum in the optimization process of $N$ and $L$. Using scattering matrix analysis[8], it can be predicted that the optimized index $N$ is determined by ka using the principle of roughly constant coupling coefficient. In this situation $N = 5$ when ka = 14.660 8. Also according to this theory $L$ is roughly a half of the beat wavelength of the $TE_{11}$ mode and the $TM_{11}$ mode in the smooth-walled waveguide with the equivalent diameter. The value of $L$ could be precisely optimized to 36.7 mm by the numerical calculations, as shown in Fig. 9.

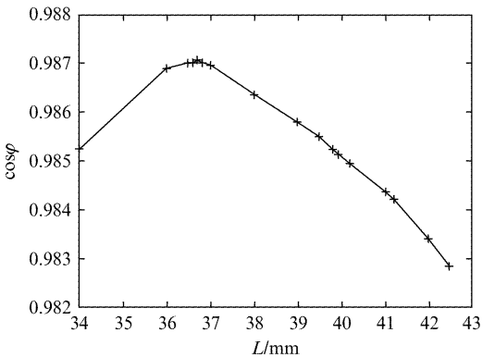


Fig. 9　The match value vs. corrugated transition length
图 9　波纹波导过渡段长度与匹配系数的关系

## 4 Design of the mirror system

The mirror system is used to transform the round symmetric Guassian beam given in Chap. 4 to the elliptical Guassian beam given in Chap. 3. At least two mirrors with distinctive curvature along different direction are required to realize such transformation according to Gaussian optics. The layout of the mirror system is shown in Fig. 10. According to the Guassian optics in part 2, $q$ parameter transformation can be written as Eq. 9 by some mathematics transformations[5]:

$$q_x = \begin{bmatrix} 1 & l_3 \\ 0 & 1 \end{bmatrix} \cdot \begin{bmatrix} 1 & 0 \\ -\dfrac{2}{R_{2x}\cos\left(\alpha + \dfrac{\theta}{2}\right)} & 1 \end{bmatrix} \cdot \begin{bmatrix} 1 & l_2 \\ 0 & 1 \end{bmatrix} \cdot \begin{bmatrix} 1 & 0 \\ -\dfrac{2}{R_{1y}\cos 45^\circ} & 1 \end{bmatrix} \cdot \begin{bmatrix} 1 & l_1 \\ 0 & 1 \end{bmatrix} * q_{x0}$$

$$q_y = \begin{bmatrix} 1 & l_3 \\ 0 & 1 \end{bmatrix} \cdot \begin{bmatrix} 1 & 0 \\ -\dfrac{2}{R_{2y}\cos\left(\alpha + \dfrac{\theta}{2}\right)} & 1 \end{bmatrix} \cdot \begin{bmatrix} 1 & l_2 \\ 0 & 1 \end{bmatrix} \cdot \begin{bmatrix} 1 & 0 \\ \dfrac{2}{R_{1y}\cos 45^\circ} & 1 \end{bmatrix} \cdot \begin{bmatrix} 1 & l_1 \\ 0 & 1 \end{bmatrix} * q_{y0} \quad , \quad (9)$$

with the definition of denotation * shown in Eq. 10:

$$A * q = \frac{A(1,1)q + A(1,2)}{A(2,1)q + A(2,2)} \quad . \quad (10)$$

It can be proved that the '*' multiplication obeys associative law of multiplication. In Eq. 9, it should be mentioned that $q_x$ and $q_y$ are complex numbers, thus four real-function equations are implied in Eq. 9. Therefore, when $l_1$, $l_2$, $l_3$ is selected, the $R_{1x}$, $R_{1y}$, $R_{2x}$, $R_{2y}$ can be derived through solving the nonlinear equations implied

in Eq. 9. With these parameters determined, the $q$ parameters along the propagation routine can be calculated via Eqs. 2 – 3. Within the range of 1.5 times of beam waist, over 99% power is included. The relationship between q parameter and beam waist can be written as Eq. 11:

$$w = \sqrt{\frac{2|q|^2}{k\mathrm{Im}q}} \quad . \quad (11)$$

By calculating 99% power-passing region, the mirror size could be determined and the selection of $l_1$, $l_2$, $l_3$ could be checked. The principle is that the curvature of the mirror should be much larger than the beam size, the mirror size should be large enough to reflect 99% microwave power at least, and the mirror cannot overlap each other in the real situation. The final parameters of the mirror system are approached by the trial and error method, as shown in Table 2. It is necessary to be mentioned that if too distinctive q parameters are to be transformed though this system, the criterion mentioned above will become hard to be satisfied.

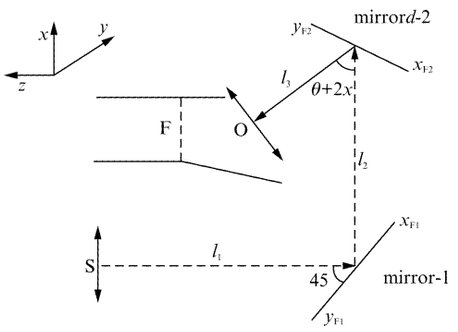


Fig. 10 Layout of the mirror system
图 10 镜面系统的布置图

**Table 2 Parameters of the mirror system**
**表 2 镜面系统的参数**

| $l_1$/mm | $l_2$/mm | $l_3$/mm | $R_{1x}$/mm | $R_{1y}$/mm | $R_{2x}$/mm | $R_{2y}$/mm |
|---|---|---|---|---|---|---|
| 25 | 27 | 15 | 62.39 | 60.64 | 52.17 | 30.45 |

## 5 Results and discussion

The whole injection system could be established with the above results. The beam aperture is also dug on the mirror system to let the electron beam through, as shown in Fig. 11. Because the beam aperture is positioned far away from the centre of the Gaussian beam(also the mirror centre), it has little effect on the transformation of the Gaussian beam except less than 1% injecting efficiency decrease comparing with the no-beam-aperture situation, according to the numeric calculations.

Add-space-open boundary is applied on this model to make the calculation more accurate. The distribution of x-component of the electric field is shown in Fig. 11. The more concrete comprehension could be achieved if Fig. 11 and Fig. 3 are checked into at the same time. With the compensation of diffraction power loss in the confocal waveguide, the mode conversion efficiency vs. frequency curve is calculated, shown in Fig. 12. For the target to maximum the efficiency at the frequency of

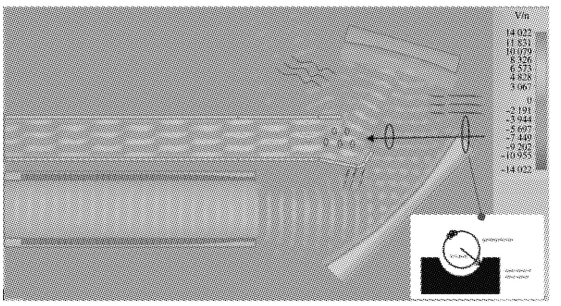


Fig. 11 Electric field distribution of the whole power coupler (wavy lines represents power loss direction, circle dots represents that the direction is vertical to paper)
图 11 整个注入系统的电场分布图.(波浪线代表输入结构的功率损失大致方位,圆圈点代表损失方向垂直纸面)

140 GHz, the relative peak point is not necessarily positioned at 140 GHz which is too close to the cut-off frequency. The power injecting efficiency at 140 GHz is around 58%. In the frequency range from 138.5 GHz to 145.3 GHz, over 50% power will be injected into the confocal waveguide. Meanwhile the proportion of reflection power is less than 10% in its over-50% frequency band.

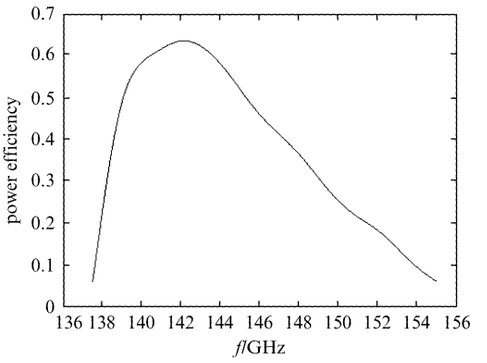


Fig. 12 Efficiency vs. frequency of quasi-optical injection
图 12 准光学注入结构的频率效率曲线

Nearly 30% power losses in free space when the Gaussian beam transmits between the exit of the corrugated waveguide and entrance of the confocal waveguide (Fig. 11). Among all the power loss, the antenna coupler takes the dominant ratio of above 25%. In the optimization of antenna coupler, a certain part of power loss is unavoidable probably because the antenna coupler's profile demonstrated in Fig. 5 is not the best choice. By modifying the antenna's shape, better efficiency performance is expected in the future research.

## 6 Conclusion

Based on theoretical analysis and numeric models. Quasi-optical launcher for 140 GHz gyrotron amplifier with frequency bandwidth of around 6.8 GHz is desiged in this paper. In contrast, my companion's earlier work to design the inserted waveguide coupler only achieves less than 2 GHz bandwidth with the larger peak efficiency by roughly 10%. As a conclusion, by sacrificing some

injection efficiency on operation frequency, a much larger bandwidth is finally accomplished. It is also evident that the quasi-optical structure could lower the probability of the oscillation instability and the reflection disturbance, also permitting larger manufacturing errors. Except from the disadvantage of machining difficulties, this quasi-optical input launcher is more compatible for 140 GHz gyrotron amplifier loaded with confocal waveguide.

The whole gyrotron amplifier is under machining.

## References

[1] Jiang Y, Chen H B, Ma G W, *et al*. Design and simulation of confocal gyro-travelling wave tube [J]. *High Power Laser and Partical Beams*. 2012, **24**(2): 403 - 406.

[2] Joye C D. A novel wideband 140 GHz gyrotron amplifier[D]. Doctorate Dissertation in Massachusetts Institute of Technology, 2004.

[3] Sirigiri J, Shapiro M, Temkin R. High-power 140 GHz quasi-optical gyrotron traveling-wave amplifier[J]. *Physics review letters*, 2003, **90**(25): 302.

[4] Hu W. Studies of novel 140 GHz gyrotrons[D]. Doctorate Dissertation in Massachusetts Institute of Technology, 1997.

[5] Zhang K Q, Li D J. *Electromagnetic theory for microwaves and optoelectronics*[M]. 2nd ed. Beijing: Publishing House of Electronics Industry, 2001.

[6] Sirigiri J S. Theory and design study of a novel quasi-optical gyrotron traveling wave amplifier[D]. Cambridge, MIT, 1999.

[7] Kowalski E J, Tax D S, Shapiro M A, *et al*. Linearly polarized modes of a corrugated metallic waveguide[J]. *IEEE Transactions on Microwave Theory and Techniques*. 2010, **58**(11): 2772 - 2779.

[8] Thumm M, Jocobs A, Ayza M S. Design of the short high-power TE11-HE11 mode converters in highly overmoded corrugated waveguides[J]. *IEEE Transactions on Microwave Theory and Techniques*. 1991, **39**(2): 301 - 308.